2010

Molecular Analysis of Primary Vapor and Char Products during Stepwise Pyrolysis of Poplar Biomass

Roger W. Jones
Iowa State University, jonesrw@ameslab.gov

Tonu Reinot
Iowa State University

John Frederick McClelland
Iowa State University

This is a manuscript of an article in *Energy Fuels* 24 (2010): 5199, doi:10.1021/ef100655n. Posted with permission.

Molecular Analysis of Primary Vapor and Char Products during Stepwise Pyrolysis of Poplar Biomass

Roger W. Jones,* Tonu Reinot, and John F. McClelland

Ames Laboratory, United States Department of Energy (U.S. DOE), and Center for Sustainable Environmental Technologies, Iowa State University, Ames, Iowa 50011

*To whom correspondence should be addressed. 109 Spedding Hall, Ames Laboratory, Iowa State University, Ames, IA 50011-3020. E-mail: jonesrw@ameslab.gov. Telephone: +1 515 294 3894.

ABSTRACT: Pyrolysis of biomass produces both pyrolysis oil and solid char. In this study, poplar has been pyrolyzed in a stepwise fashion over a series of temperatures from 200 to 500 °C, and both the primary products contributing to pyrolysis oil and the changes in the pyrolyzing poplar surface leading toward char have been characterized at each step. The primary products were identified by direct analysis in real time (DART) mass spectrometry, and the changes in the poplar surface were monitored using Fourier transform infrared (FTIR) photoacoustic spectroscopy, with a sampling depth of a few micrometers. The primary products from pyrolyzing cellulose, xylan, and lignin under similar conditions were also characterized to identify the sources of the poplar products.

Introduction

Lignocellulosic biomass is a promising source for both energy and chemical products because of its abundance and renewability. Pyrolysis is an important process for converting biomass into a liquid feedstock for fuel and chemicals. Recently, there has also been interest in the char formed during pyrolysis, which can be used to improve soil fertility and sequester carbon. During pyrolysis at low or moderate heating rates, biomass decomposes in stages, with moisture evolution first, hemicellulose decomposition second, then cellulose decomposition, and lignin decomposing over a wide temperature range, finishing last.[1-4] Understanding the thermal decomposition behavior during pyrolysis is crucial to controlling the end-product composition, but gaining an understanding is complicated because pyrolysis proceeds by a complex series of reactions that depends upon the chemical composition and physical structure of the biomass and the pyrolysis conditions.[1,2]

Our objectives in the present study were to observe both the primary pyrolysis product vapors prior to the complex series of secondary pyrolysis reactions and the corresponding chemical changes of the pyrolyzing biomass surface as it chars. Two analytical methods were used in the study: direct analysis in real time mass spectrometry (DART-MS) was used to identify and measure the pyrolysis products,[5,6] and Fourier transform infrared photoacoustic spectroscopy (FTIR-PAS) was used to characterize the chemical changes on the biomass surface.[7-11] The experiments used hybrid poplar because it is a fast growing biomass of interest as a pyrolysis feedstock.

The DART-MS measurements used a heated stream of electronically excited (metastable) helium atoms to ionize primary pyrolysis products, so that they could be analyzed by the mass spectrometer. This method permitted the analysis of primary pyrolysis products as they formed and before significant formation of secondary products. DART-MS has good time resolution, so each temperature step in the pyrolysis protocol was well resolved. Small amounts of very finely ground poplar were used for the DART-MS determination of pyrolysis products. Using small amounts of biomass assured that the material was uniformly heated. Fine grinding assured that decomposition products formed within a

biomass particle had only a short distance to diffuse before escaping the particle; therefore, secondary reactions with the biomass surface were minimized.

Experimental Section

To study the changes within wood as it chars during its pyrolysis, we pyrolyzed a 1.8 mm thick slice of hybrid poplar in a step-wise fashion by exposing it to a stream of hot nitrogen for a series of 90 s periods, with each successive period being at a higher temperature than the previous period. The poplar sample was placed in a small, air-free chamber through which a 23 L/min flow of heated nitrogen passed. For the first exposure, the nitrogen was at 200 °C. For each successive exposure, the nitrogen was 25 °C hotter than the previous exposure, up to 300 °C. Beyond that point, each successive exposure was 10 °C hotter than the previous, up to 500 °C.

After each exposure, the sample was cooled to room temperature and its mid-infrared spectrum was recorded using FTIR-PAS.[7,8] A MTEC Photoacoustics PAC 300 detector was mounted in a Digilab FTS 7000 FTIR spectrometer for the analysis. The sample chamber in the detector has a 1 cm interior diameter and a window at the top through which the infrared beam from the spectrometer enters. The poplar sample was placed face up in the detector. Because the pyrolysis proceeded slightly faster at the edge of the poplar slab, a metal ring was placed atop the slab, so that only the central, most uniformly pyrolyzed portion of the face of the sample was exposed to the infrared beam and analyzed. The detector was purged with helium immediately prior to spectrum acquisition to minimize interference from water vapor and carbon dioxide, which have strong mid-infrared absorptions. A small amount of magnesium perchlorate desiccant was placed beneath the sample to eliminate any water vapor that evolved from the sample during the analysis. Spectra were taken with 8 cm^{-1} resolution at a 40 kHz scanning speed (i.e., at a 40 kHz laser-fringe modulation frequency by the spectrometer interferometer), with the co-addition of 8192 scans.

Unlike conventional transmission spectroscopy, FTIR-PAS does not require the infrared radiation to pass completely through the sample; therefore, it works well with opaque materials, such as wood, even after it begins to darken during char formation. FTIR-PAS has been used before for the analysis of char.[12] PAS directly measures infrared absorbance by detecting the energy deposited in the sample by the infrared radiation. When the radiation is absorbed in the sample, the deposited heat diffuses to the sample surface and transfers to the surrounding helium gas. The resulting temperature change of the gas produces a pressure change proportional to the light absorption, which is detected by a sensitive microphone in the PAS detector. Because of the time required for thermal diffusion, PAS is a sample-depth-sensitive technique.[7,8] The faster the spectrometer scans, the faster it modulates the infrared beam; thus, there is less time for heat to diffuse out from the sample, and the absorption in the sample must occur nearer to the surface for the detector microphone to sense it. The sensing depth of PAS depends upon the thermal diffusivity of the sample, the spectrometer modulation frequency, and the wavenumber position within the spectrum.[7,8] On the basis of a thermal diffusivity of 2.17×10^{-7} m^2/s for poplar,[13] the 40 kHz scanning speed used here corresponds to a sensing depth of 3–8 μm for the unaltered poplar over the 4000–400 cm^{-1} range of the mid-infrared spectra. The sensing depth changes as the wood chars because the high absorption coefficient of the char gradually reduces the sampling depth across the entire spectral range.

To study the volatile products produced by poplar and its components during pyrolysis, we used a JMS-100TLC (AccuTOF) time-of-flight mass spectrometer (JEOL USA, Peabody, MA) with a DART SVP ion source (IonSense, Saugus, MA) that provides sample ionization at atmospheric pressure external to the mass spectrometer. The DART ion source produces a stream of hot, metastable (i.e., electronically excited) helium atoms.[5] The stream is aimed across an open-air gap at the inlet of the mass spectrometer. The metastable atoms either ionize the pyrolysis vapors directly or interact with moisture to produce ionized water clusters, $(H_2O)_nH_3O^+$, which then ionize the vapors. An in-house-built, small-volume (~0.2 mL) pyrolysis chamber made of Teflon was inserted between the DART source and the mass spectrometer inlet, as shown schematically in Figure 1. The chamber housing fitted

loosely between the DART source and the spectrometer inlet so that the chamber remained at ambient pressure. In addition to the helium-gas sampling stream from the DART source passing through the pyrolysis chamber, nitrogen actively purged the chamber to keep oxygen out. The oxygen peak (O_2^+ at *m*/*z* 31.98) was monitored, and the purge gas flow was adjusted to eliminate it. Within the pyrolysis chamber was a Heraeus MSP 769 multisensor platform, which incorporates a heating element and a platinum thin-film temperature sensor and which acted as a micropyrolyzer stage. The micropyrolyzer has a very high heating rate and can ramp to 500 °C in 1.1 s. Its temperature was computer controlled and stabilized to better than 0.1 °C.

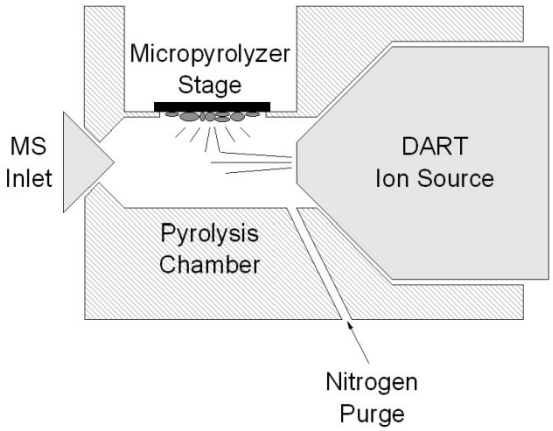

Figure 1. Schematic of the pyrolysis chamber used to study the primary volatile pyrolysis products. The chamber fits in the gap between the DART ion source and the mass spectrometer inlet.

Hybrid poplar sawdust was ground using an in-house, motorized, ground-glass, laboratory mill into a sufficiently fine pulp that poplar particles stayed suspended in water for over 1 h. A total of 1 μL of the poplar suspension contained approximately 1 μg of wood. For each pyrolysis experiment, a well-diluted 1 μL droplet of suspension was placed onto the micropyrolyzer surface and air-dried to form a visually uniform thin layer. Grinding the sample into very small particles was performed to allow for the preparation of very thin and uniform sample films with low thermal mass and good thermal contact with the micropyrolyzer and thereby improve pyrolysis uniformity, repeatability, and temperature control. The pre-pyrolysis temperature of the sample in the chamber was approximately 130 °C because the DART source gas was heated to 250 °C.

Cellulose (20 μm microcrystalline powder), alkali lignin, and xylan (all from Sigma-Aldrich) were also suspended in water and placed on the micropyrolyzer for pyrolysis studies. The cellulose and xylan were both ground in a manner similar to the poplar. The lignin particle size was smaller than 5 μm; therefore, the lignin was used as received.

Two different heating protocols were used. In a single-step pyrolysis, the micropyrolyzer temperature was raised as fast as possible to the target temperature and then kept stable at it, avoiding temperature oscillations. In multi-step pyrolysis, the micropyrolyzer temperature was increased by constant temperature increments at constant time intervals; thus, the temperature had a staircase-like time profile.

The mass spectrometer was operated in positive-ion mode. The inlet orifice (orifice 1) was set to a potential of 20 V and a temperature of 80 °C. The ring lens and orifice 2 potential parameters were each set to 3 V. The radio-frequency (RF) ion guide potential was 400 V. Data acquisition was set to acquire the *m*/*z* 40–700 range. Accordingly, the low-molecular-weight gases produced during the pyrolysis (e.g., CO, CH_4, and C_2H_4) were not observed. In addition, carbon dioxide was not observed by DART because of its low proton affinity. The DART ion source was operated with helium gas at a flow rate of 4 ± 0.3 L/min. The ion-source heater was set to 400 °C, but the actual temperature of the gas at the micropyrolyzer was 250 ± 5 °C. The grid electrode at the exit of the source was set to 530 V. Exact

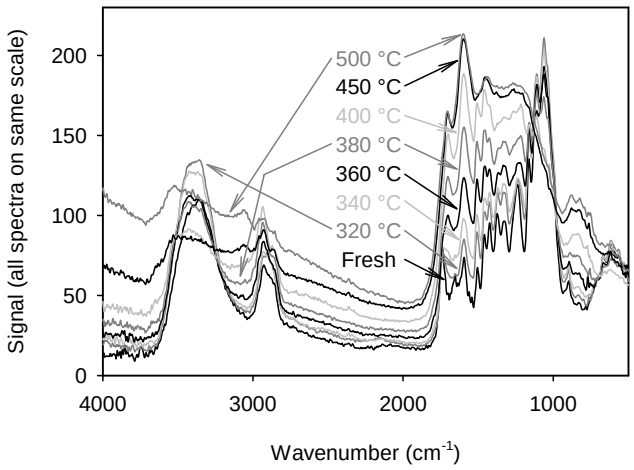

Figure 2. Selected FTIR-PAS spectra of a poplar slab during its stepwise pyrolysis. The temperature of the pyrolysis step preceding acquisition of each spectrum is indicated. The spectra are all shown on the same vertical scale without offsets.

mass calibration was accomplished by including a mass spectrum of neat polyethylene glycol (PEG 600). A melting point tube dipped in PEG was passed in front of the DART ion source to produce the calibration spectrum. The mass calibration was accurate to within 0.003 u. DART spectra are dominated by protonated molecules, $[M + H]^+$, where M is the neutral molecule; therefore, the accurate mass calibration allowed identities to be assigned to many individual peaks in the mass spectra. Unless otherwise indicated, all identified spectrum peaks are $[M + H]^+$ species.

Results and Discussion

FTIR Spectra of Pyrolyzing Poplar. A thin slab of poplar was pyrolyzed stepwise by exposing it to a stream of hot nitrogen for numerous 90 s periods. We began with an exposure to 200 °C nitrogen, proceeded in 25 °C steps up to 300 °C, and then used 10 °C steps up to 500 °C. After each exposure, a FTIR-PAS spectrum of the poplar surface was acquired. Figure 2 shows a series of these spectra after selected temperature steps during the pyrolysis. Every absorption feature in the spectrum is altered by the pyrolysis. Most of the many absorption peaks of the fresh wood disappear and are replaced by a few broader absorptions from pyrolysis products. In addition, a broad-spectrum, background absorption begins to push the baseline of the spectra upward, starting at roughly 340 °C. This baseline shift is shown more clearly in Figure 3. This rising baseline indicates the formation of a carbon-black char, which absorbs all wavelengths of infrared light. The char also intensely scatters the infrared light, which produces the sloped baseline of the higher temperature spectra in Figure 2.

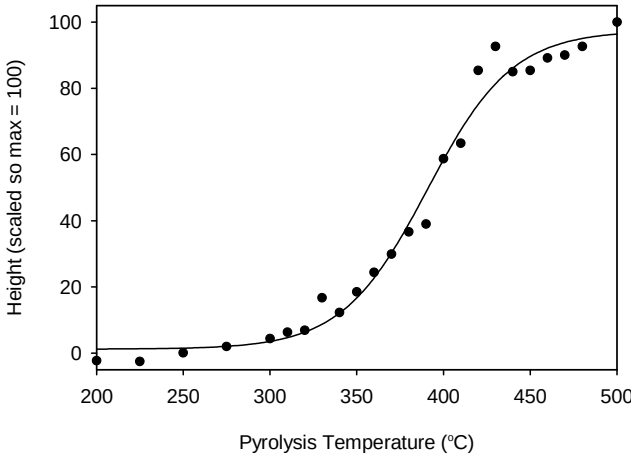

Figure 3. Baseline level of spectra at 2002 cm^{-1}. This increase indicates the formation of carbon char as the pyrolysis temperature rises.

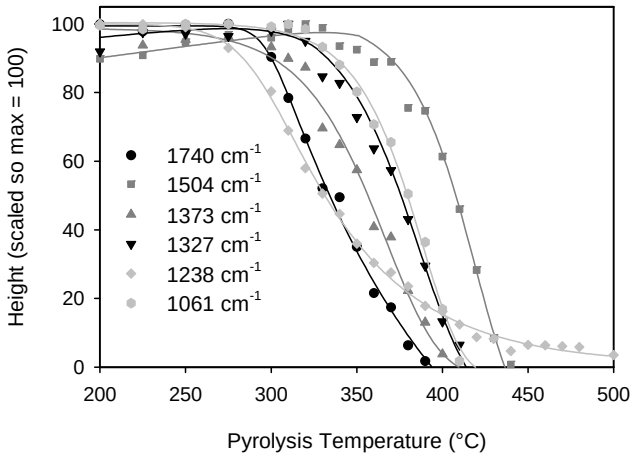

Figure 4. Pyrolysis temperature dependence of absorption peaks present in the fresh-wood spectrum. The locations of the peaks are given in the key within the figure. Data for each peak have been scaled to 100 at the greatest intensity.

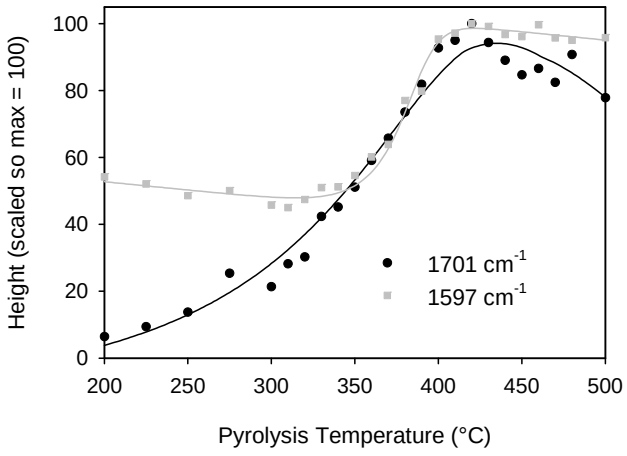

Figure 5. Pyrolysis temperature dependence of absorption peaks still present in the char at 500 °C. Peak locations are given in the key within the figure. Data for each peak have been scaled to 100 at the greatest intensity.

The sources of the absorption peaks in fresh wood have been identified by previous researchers.[10] The temperature-dependent behavior of the peaks in Figure 2 spectra can therefore be related to the chemical changes occurring during the pyrolysis. Figures 4–6 show the temperature dependences of selected peaks, and the sources of these absorption peaks are listed in Table 1.

All of the peaks plotted in Figure 4 are wood absorptions that diminish to nothing or nearly nothing as the pyrolysis temperature rises. The differing peaks decrease in size at different temperatures. The 1740 cm^{-1} carbonyl-bond peak from hemicellulose is the first to disappear. In order of increasing temperature, it is followed by the 1373 cm^{-1} peak from both cellulose and hemicellulose, the 1327 cm^{-1} peak from cellulose, the 1061 cm^{-1} peak from cellulose and hemicellulose, and the 1504 cm^{-1} peak from lignin. This order of disappearance is consistent with the findings of previous researchers, who observed that hemicellulose decomposed in the lowest pyrolysis-temperature range, cellulose decomposed in a somewhat higher (but overlapping) range, and lignin was the most resistant, decomposing only at higher temperatures.[2]

One peak plotted in Figure 4 does not follow this simple pattern. The 1238 cm^{-1} peak is the first to begin decreasing in size as the temperature rises, but it decreases so slowly that it is still present when the 1504 cm^{-1} lignin peak drops to zero. This peak has been identified as having a mixed origin. It comes from both syringyl nuclei in lignin and from C=O bonds in hemicellulose.[10] Its unusual temperature decay is consistent with its mixed parentage. Its decrease in intensity at low temperatures is consistent with the hemicellulose portion of the feature, but its continued presence at relatively high temperatures is consistent with its lignin source.

In contrast to those in Figure 4, the two peaks plotted in Figure 5 grow with increasing temperature. The 1597 cm^{-1} peak arises from an aromatic ring stretch in lignin in the fresh wood. The species causing the band to increase as the wood chars is not certain, but it is likely to be an additional aromatic ring stretch from other species. The aromaticity of the char is known to increase because both oxygen and hydrogen are lost from the char at a faster rate than carbon.[15,16] The 1701 cm^{-1} band, in contrast, is not present in the fresh wood. Its location is consistent with a carbonyl (C=O) structure, although the specific form has not been identified.

The spectral region above 2000 cm^{-1} has far fewer absorption peaks than the region below 2000 cm^{-1}, and those peaks tend to be from multiple origins rather than from just one of the cellulose, hemicellulose, and lignin components. Nevertheless, those high-wavenumber peaks do provide useful information. The temperature dependences for these peaks are plotted in Figure 6 and are not

particularly similar to those shown in Figures 4 and 5. The two bands 3356 and 3522 cm^{-1} have similar temperature dependences, both peaking near 300 °C and then dropping off by at least half by 400 °C. Both of these bands arise from stretching of O–H bonds. The 3522 cm^{-1} feature corresponds to O–H that is hydrogen-bonded to aromatic species, while the 3356 cm^{-1} feature can involve hydrogen bonding to various O and H species. Hydrogen bonding is stronger to nearby O and H atoms than to nearby C atoms; therefore, we can infer from the slower drop off of the 3522 cm^{-1} band at high temperature that the pyrolysis has eliminated much of the O and H atoms initially present in the wood, leaving principally an aromatic structure.[15,16]

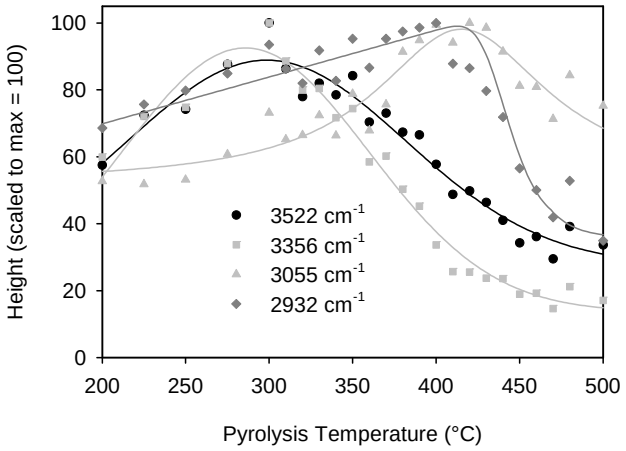

Figure 6. Pyrolysis temperature dependence of high-wavenumber peaks. Peak locations are given in the key within the figure. Data for each peak have been scaled to 100 at greatest intensity.

The other two bands in Figure 6, 3055 and 2932 cm^{-1}, both reach a peak near 400 °C, although the 2932 cm^{-1} band rises to that peak slower and drops from it faster than the 3052 cm^{-1} band. Both of these bands come from stretching of C–H bonds, but those contributing to the 3052 cm^{-1} peak are in aromatic structures, while those contributing to the 2932 cm^{-1} peak are in aliphatic structures. The low-temperature rise of both of these indicates an increase in C–H bonds as oxygen is expelled from the wood. The smaller rise to 400 °C and greater fall off from there of the aliphatic peak indicates that the aliphatic structures are decomposing more readily than the aromatic structures. This is consistent with the previously mentioned observation that the aromaticity of pyrolysis chars increases with the temperature. This is also consistent with the behavior of the aromatic 1597 cm^{-1} peak discussed above.

DART-MS Studies of Pyrolysis Products. We examined the pyrolysis of hybrid poplar wood by DART-MS using the micropyrolyzer chamber described in the Experimental Section. The experiments included pyrolysis at a single temperature and stepwise pyrolysis at a series of temperatures to delineate the series of steps through which the pyrolysis proceeds. We have also examined the products from pyrolysis of the individual wood components (cellulose, hemicellulose, and lignin). The pyrolysis chamber was positioned between the DART ion source and the inlet to the mass spectrometer. Approximately 1 μg of poplar was placed on the micropyrolyzer surface and air-dried for each experiment. Two different heating protocols were used. In a single-step pyrolysis, the sample temperature was rapidly raised to the target temperature and then held there. In multi-step pyrolysis, the sample temperature was increased by constant temperature increments at constant time intervals; thus, the temperature formed a staircase-like time profile.

Single-Step Pyrolysis at 500 °C. Samples of poplar wood and of cellulose, xylan, and lignin were pyrolyzed at 500 °C. Figure 7 shows the time evolution of the poplar pyrolysis products in the mass range m/z = 60–400 u. Most of the products rise rapidly to a peak and then taper off, but a few, such as m/z 325 and 342, have double-peaked time profiles consisting of a quick, early peak followed by a much slower second peak.

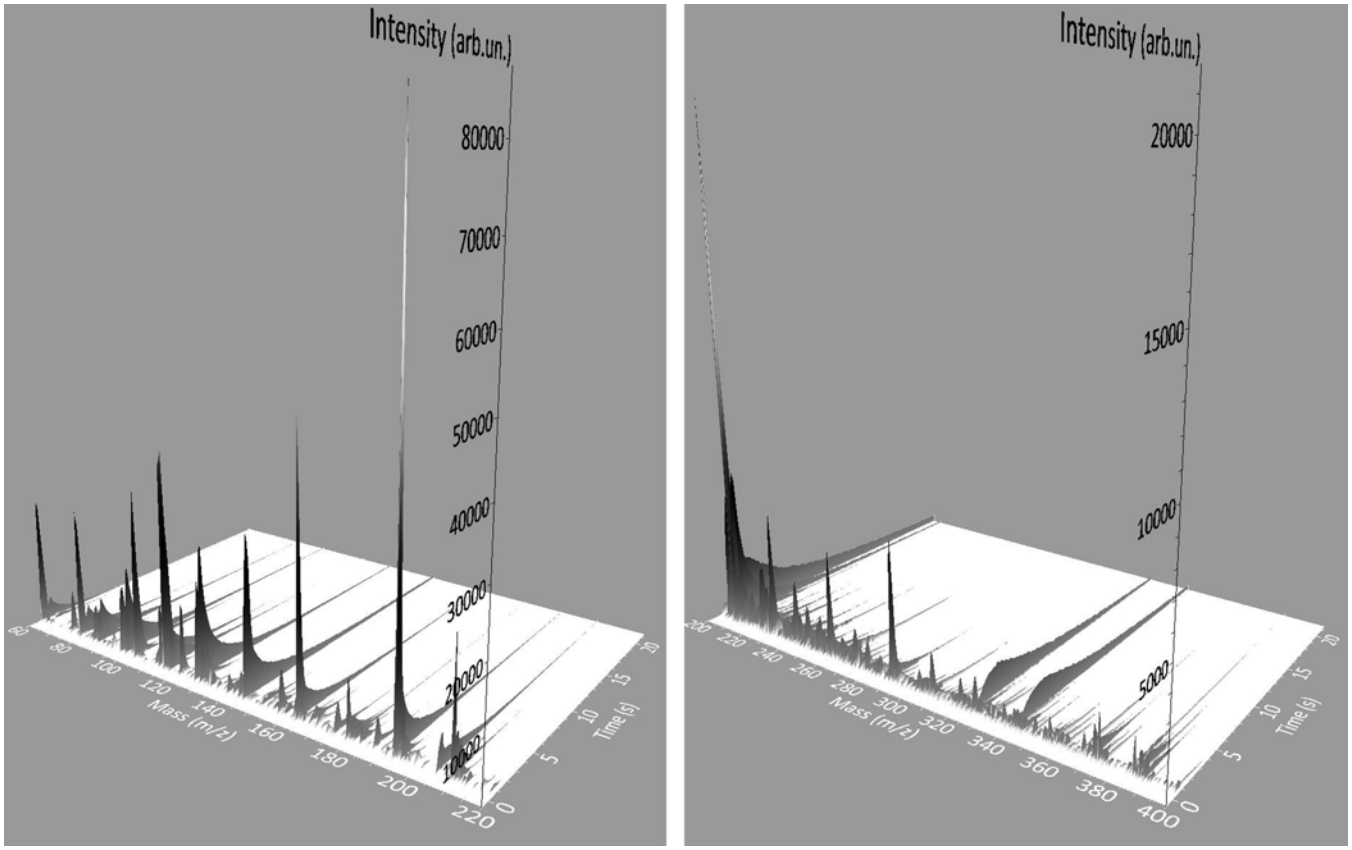

Figure 7. Hybrid poplar pyrolysis at T = 500 °C. Left: *m*/*z* 40 to 220. Right: *m*/*z* 200 to 400, with the intensity scale expanded ×4. The most abundant peaks are listed in Table 2.

Table 2 lists all of the major peaks observed in the pyrolysis of poplar at 500 °C. The table also lists the observed product ions from the 500 °C pyrolysis of the separate wood components that correspond to the poplar-wood product ions. All of these products can be at least tentatively identified.

The *m*/*z* 61 ion is probably protonated acetic acid ($C_2H_4O_2$), which many have observed as a pyrolysis product,[17-19] although researchers have also observed the isomers glycolaldehyde in polysaccharide pyrolysis[20] and methyl formate in wood pyrolysis.[18] The ion is produced in the pyrolysis of all three of the wood components. The *m*/*z* 79 ion is protonated $C_2H_6O_3$, but this molecule is not a stable species that can be observed by the slow chromatographic methods that predominate in literature reports on separating and identifying pyrolysis products. Our direct analysis by DART-MS can potentially observe less stable products. The most stable species of the $C_2H_6O_3$ formula could come from are an ethanetriol [$HOCH_2–CH(OH)_2$ or $CH_3–C(OH)_3$] or a dimethyl ether diol [$HOCH_2–O–CH_2OH$ or $CH_3–O–CH(OH)_2$]. These correspond approximately to fragments of the sugar base units that make up polysaccharides and fragments of lignin structures; therefore, they are plausible initial products from all three of the wood components.

The *m*/*z* 85, 97, and 99 ions can come from polysaccharide pyrolysis, and consistent with that, we observe them from the pyrolysis of both cellulose and xylan but not from lignin. The *m*/*z* 85 ion is certainly 2(5*H*)-furanone ($C_4H_4O_2$),[17,20-22] although the isomer 2(3*H*)-furanone has also been produced in wood pyrolysis and may be contributing to the observed ion.[23] The *m*/*z* 97 ion has usually been identified as 2-furaldehyde ($C_5H_4O_2$, commonly called furfural),[17,18,20,22-25] although $C_5H_4O_2$ has also been identified as the isomers 3-furaldehyde[21,24] and 4-cyclopentene-1,3-dione.[24] The *m*/*z* 99 ion comes from $C_5H_6O_2$, which has usually been determined to be furfuryl alcohol,[18,19,24] but it has also been identified as one of the isomers 3-, 4-, and 5-methyl-2(5*H*)-furanone in wood pyrolysis.[20-23]

The *m*/*z* 103 ion is protonated $C_4H_6O_3$, but this formula appears to come from two different isomeric compounds. We observe it as a product from both cellulose and xylan. Acetic anhydride has been observed as a product of hemicellulose pyrolysis;[17] therefore, it may be the product from xylan,

and methyl pyruvate is an observed product of wood pyrolysis;[23] therefore, it may be the product from cellulose.

We observe the *m*/*z* 111 ion from the pyrolysis of poplar and all three of the wood components. The ion is protonated $C_6H_6O_2$, but this is probably more than one species. It may be pyrocatechol, which is observed in the pyrolysis of wood, hemicellulose components including xylan, and lignin;[17-19,21,23,26] it may be 2-acetyl furan, which is observed from both wood and cellulose;[17,22,23] it may be 5-methylfurfural coming from cellulose;[17,18,24,26] it may be hydroquinone, which comes from xylan;[17,26] it could be 2-furoic acid methyl ester from polysaccharides;[24] and it may be various dihydroxybenzenes.[26]

We observed the *m*/*z* 113, 115, and 127 ions in the pyrolysis of poplar, cellulose and xylan. The *m*/*z* 113 ion is protonated $C_5H_4O_3$ and is probably 2-furoic acid, which has been observed in the pyrolysis of xylan derivatives,[27] although it has also been identified as 2*H*-pyran-2,6(3*H*)-dione from cellulose.[22] The *m*/*z* 115 ion is $C_5H_6O_3$, which may be either dihydro-2-(hydroxymethylene)-3(2*H*)-furanone or 4-hydroxy-5,6-dihydro-(2*H*)-pyran-2-one. Both of these have been observed in the pyrolysis of polysaccharides.[20,22,25] The *m*/*z* 127 ion comes from $C_6H_6O_3$, but three different species with that formula have been observed in polysaccharide pyrolysis. They are 5-hydroxymethylfurfural, which is the most widely observed of the three, 3-furancarboxylic acid methyl ester, and levoglucosenone.[17,18,22,24]

The ion at *m*/*z* 145 is protonated $C_6H_8O_4$ and is probably the dianhydrosugar 1,4:3,6-dianhydro-α-D-glucopyranose, which several groups have identified as a cellulose pyrolysis product,[17,18,22,24] although the isomeric dianhydrosugar 1,4:3,6-dianhydromannofuranose has also been observed.[24]

The *m*/*z* 163 ion could also have two origins. At an exact mass of 163.061 u would be protonated levoglucosan, $[C_6H_{10}O_5 + H]^+$, and levoglucosan is often a major product of polysaccharide pyrolysis.[17,18,24] Nearby at 163.076 u would be an ion having the formula $[C_{10}H_{10}O_2 + H]^+$, which is a product of lignin pyrolysis. It has been observed as an unidentified lignin product by Oudia et al.[28] and as 4-propynylguaiacol by Ralph and Hatfield.[25] We observe an *m*/*z* 163 ion as a product in the pyrolysis of all three components: cellulose, hemicellulose, and lignin. The exact masses observed for the ion in the wood and lignin pyrolysis are above 163.07 u, which is much closer to the lignin product than to levoglucosan. The ions that we observe in the pyrolysis of cellulose and xylan, however, are closer to the *m*/*z* of protonated levoglucosan. We therefore believe that the wood product comes at least mostly from lignin, although we are observing levoglucosan in the pyrolysis of cellulose and xylan.

Although lignin is an amorphous material, it can be described as a cross-linked polyphenolic network built principally upon two phenols: 2-methoxyphenol ($C_7H_8O_2$, commonly called guaiacol) and 2,6-dimethoxyphenol ($C_8H_{10}O_3$, commonly called syringol). For softwoods, such as poplar, guaiacol dominates. Coniferaldehyde ($C_{10}H_{10}O_3$), which is responsible for the *m*/*z* 179 ion,[20,22,24,29] could also be called 4-propenalguaiacol. We observe it coming from both poplar and lignin.

Nearly all of the ions listed in Table 2 are protonated molecules. One likely exception is *m*/*z* 180, corresponding to $C_{10}H_{12}O_3^+$. The species $C_{10}H_{11}O_3$ has not been observed as an important product in the pyrolysis of wood; therefore, the observed ion is probably not its protonated counterpart. Instead, the observed species is probably the ionized product molecule $C_{10}H_{12}O_3$. This formula has been observed in wood pyrolysis and identified as coniferyl alcohol, a guaiacol derivative.[23]

There is some question about the identity of the *m*/*z* 193 product ion, which corresponds to the formula $[C_{11}H_{12}O_3 + H]^+$. Literature sources identify this as 4-(4-hydroxy-3-methoxyphenyl)-3-buten-2-one, a product of lignin pyrolysis.[24,30] We, however, did not observe an *m*/*z* 193 ion in the study of lignin pyrolysis discussed below. Instead, we detected it as a minor product of xylan pyrolysis. We therefore cannot confirm the attribution to lignin given in the literature. Our lack of detection in the lignin study may be the result of the source of lignin used in the study. We have used alkali lignin (from Aldrich) in all of our studies. The exact chemical nature of lignin is dependent upon the method by which it is isolated from its natural source, and this may affect the reaction process during pyrolysis.[26,31]

We have not been able to identify the *m*/*z* 205.070 ion observed in the poplar pyrolysis, which is also present in cellulose pyrolysis. The two formulas closest to this mass are $[C_8H_{12}O_6 + H]^+$ at 205.071

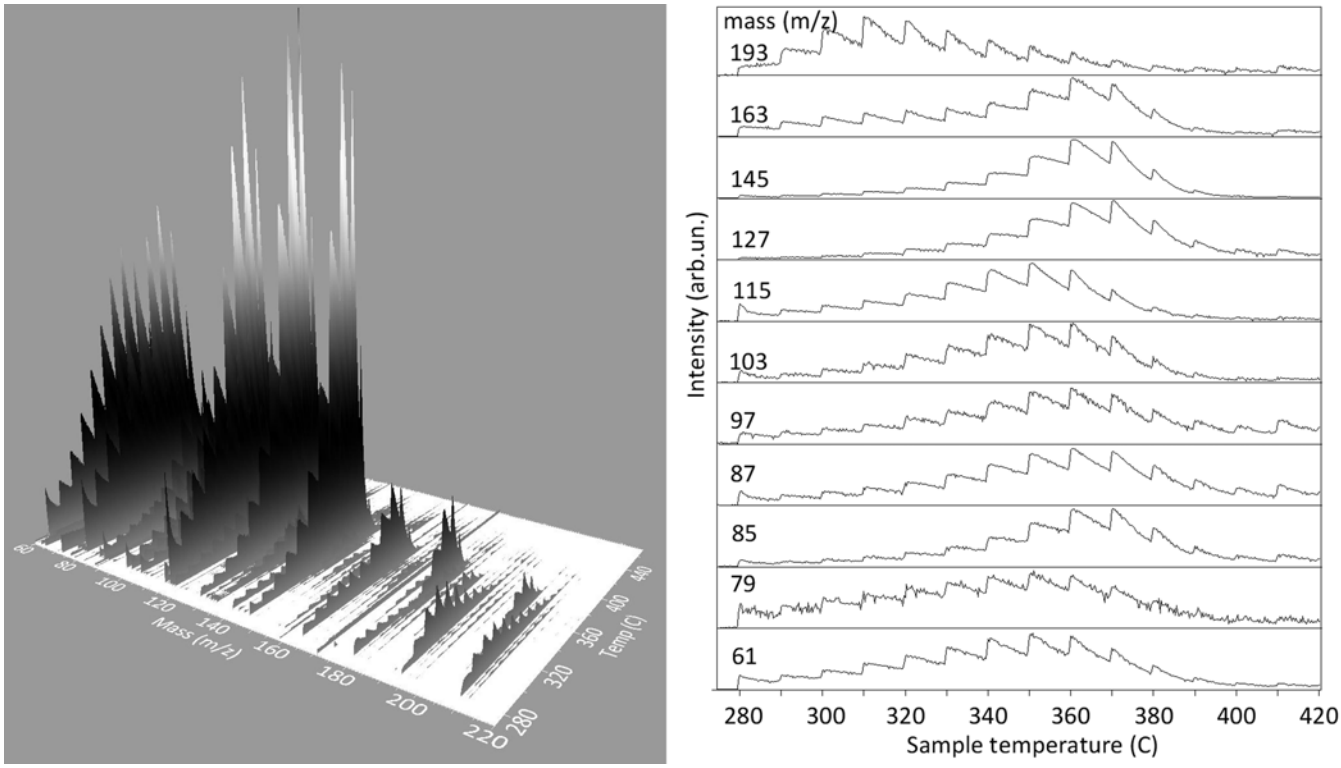

Figure 8. Left: Hybrid poplar multi-step pyrolysis from 280 to 460 °C with steps of 10 °C lasting 20 s each. Right: Individual time profiles of the most abundant pyrolysis products. The integer *m*/*z* value is indicated for each profile.

u and $[C_{15}H_8O + H]^+$ at 205.065 u, but neither of these corresponds to a pyrolysis product identified in the literature.

The *m*/*z* 209 ion comes from $C_{11}H_{12}O_4$. It could be either sinapaldehyde or 4-oxyallylsyringol, two isomers that are both products that others have observed in lignin pyrolysis,[22,24,25] although we did not in our experiments. This may again be the result of our using alkali lignin.

The ions at *m*/*z* 325 and 342 are different from the others in that they show a strong but slow second production pulse a few seconds into the pyrolysis process. The *m*/*z* 325 ion is protonated cellobiosan [or 4-*O*-(*β*-D-glucopyranosyl)-1,6-anhydro-*β*-D-glucopyranose]. Cellobiosan is essentially a dimer consisting of one glucose ring and the anhydrosugar levoglucosan, and it has been identified as a pyrolysis product of cellulose.[32] The *m*/*z* 342 ion is ionized (not protonated) $C_{16}H_{22}O_8$. It is not certain what this species is, but its likeliest identity is coniferin, which, similar to cellobiosan, is a glucose ring attached to a second ring; however, the second ring in this case is that of coniferyl alcohol rather than a sugar derivative. Glucosides, which are the combination of a glucose ring with a non-carbohydrate moiety, are common in plant material.

Stepwise Pyrolysis. Multi-step pyrolysis runs were performed using 20 s long, 10 °C steps for poplar and 40 s long, 20 °C steps for the wood components cellulose, xylan, and lignin. The time evolution of the product mass spectrum in the multi-step pyrolysis of poplar is shown in Figure 8. Notice that the peak-production temperature varies widely among the ions shown. The stepwise pyrolysis favors low-mass decomposition products, when compared to the 500 °C pyrolysis described above. The most abundant component in single-step pyrolysis, *m*/*z* = 193, is much lower in concentration in the slower and less violent step-wise pyrolysis.

The individual time profiles of the principal product ions from stepwise poplar pyrolysis are shown in the right half of Figure 8. These are all protonated molecules, and all but one are species discussed above in the single-step pyrolysis. Acetic acid produces the ion at *m*/*z* 61. An ethanetriol or a dimethyl ether diol is the ion at *m*/*z* 79. 2(5*H*)-Furanone is at *m*/*z* 85. *m*/*z* 97 comes from 2-furaldehyde (or possibly 3-furaldehyde or 4-cyclopentene-1,3-dione). Acetic anhydride or methyl pyruvate is *m*/*z* 103.

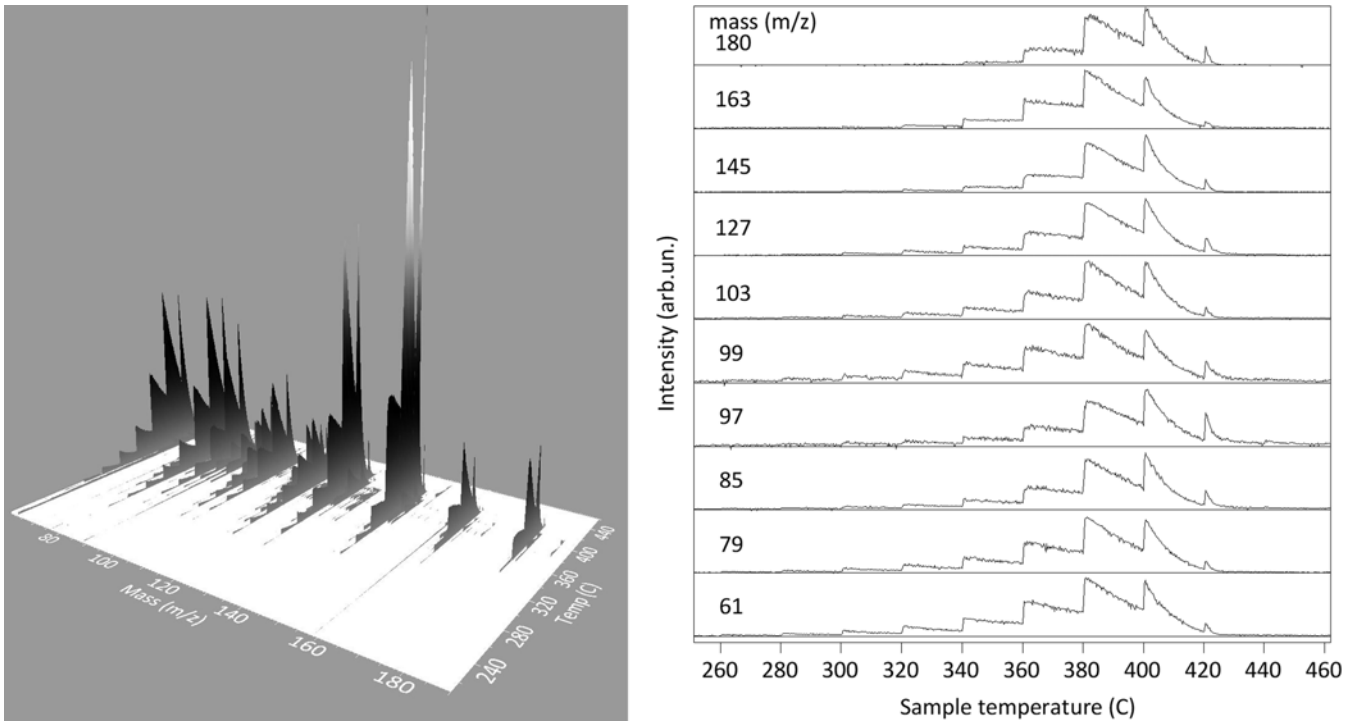

Figure 9. Left: Cellulose multi-step pyrolysis from 220 to 460 °C with steps of 20 °C lasting 40 s each. Right: Individual time profiles of the most abundant pyrolysis products. The integer *m*/*z* value is indicated for each profile.

m/*z* 115 is dihydro-2-(hydroxymethylene)-3(2*H*)-furanone or 4-hydroxy-5,6-dihydro-(2*H*)-pyran-2-one. 5-Hydroxymethylfurfural (or possibly 3-furancarboxylic acid methyl ester or levoglucosenone) is *m*/*z* 127. *m*/*z* 145 is probably 1,4:3,6-dianhydro-α-D-glucopyranose. *m*/*z* 163 is a combination of levoglucosan and the product of lignin pyrolysis $C_{10}H_{10}O_2$. As discussed for the 500 °C pyrolysis, the identity of the *m*/*z* 193 ion is uncertain. Literature sources identify it as 4-(4-hydroxy-3-methoxyphenyl)-3-buten-2-one coming from lignin,[24,30] but our experiments do not confirm that. The one product not previously discussed, *m*/*z* 87, comes from 2,3-dihydro-1,4-dioxin ($C_4H_6O_2$),[17] which we also observe as a xylan pyrolysis product.

The *m*/*z* 193 ion is produced at a relatively low temperature, with production peaking at 310 °C. The other ions shown on the right in Figure 8 have their peak production between 350 and 370 °C. It is interesting to note that the *m*/*z* 325 and 342 ions observed in the one-step, 500 °C pyrolysis are essentially absent in the multi-step pyrolysis. These species are both two-ring carbohydrate derivatives. Apparently the temperature steps in the multi-step process are too gentle to produce such large species whole. Chaiwat et al.[32] have noted that the yield of cellobiosan, which gives rise to the *m*/*z* 325 ion, is substantially greater in flash pyrolysis than it is in a pyrolysis where the temperature is raised more slowly.

Figure 9 shows the production profiles of the main products from the stepwise pyrolysis of cellulose. It is noteworthy that the most abundant cellulose pyrolysis products have very similar temperature profiles. This implies that the decomposition occurs from a single starting point, which is consistent with the uniform nature of cellulose. All of the species in Figure 9 have previously been discussed in the 500 °C pyrolysis of poplar, and all but *m*/*z* 99 and 180 are major products of the stepwise pyrolysis of poplar shown in the right half of Figure 8. The *m*/*z* 61 ion is acetic acid. An ethanetriol or a dimethyl ether diol is the ion at m/z 79. 2(5*H*)-Furanone is *m*/*z* 85. *m*/*z* 97 comes from 2-furaldehyde (or possibly 3-furaldehyde and 4-cyclopentene-1,3-dione). The *m*/*z* 99 ion is probably furfuryl alcohol. Acetic anhydride or methyl pyruvate is *m*/*z* 103. 5-Hydroxymethylfurfural (or possibly 3-furancarboxylic acid methyl ester or levoglucosenone) is *m*/*z* 127. *m*/*z* 145 is probably

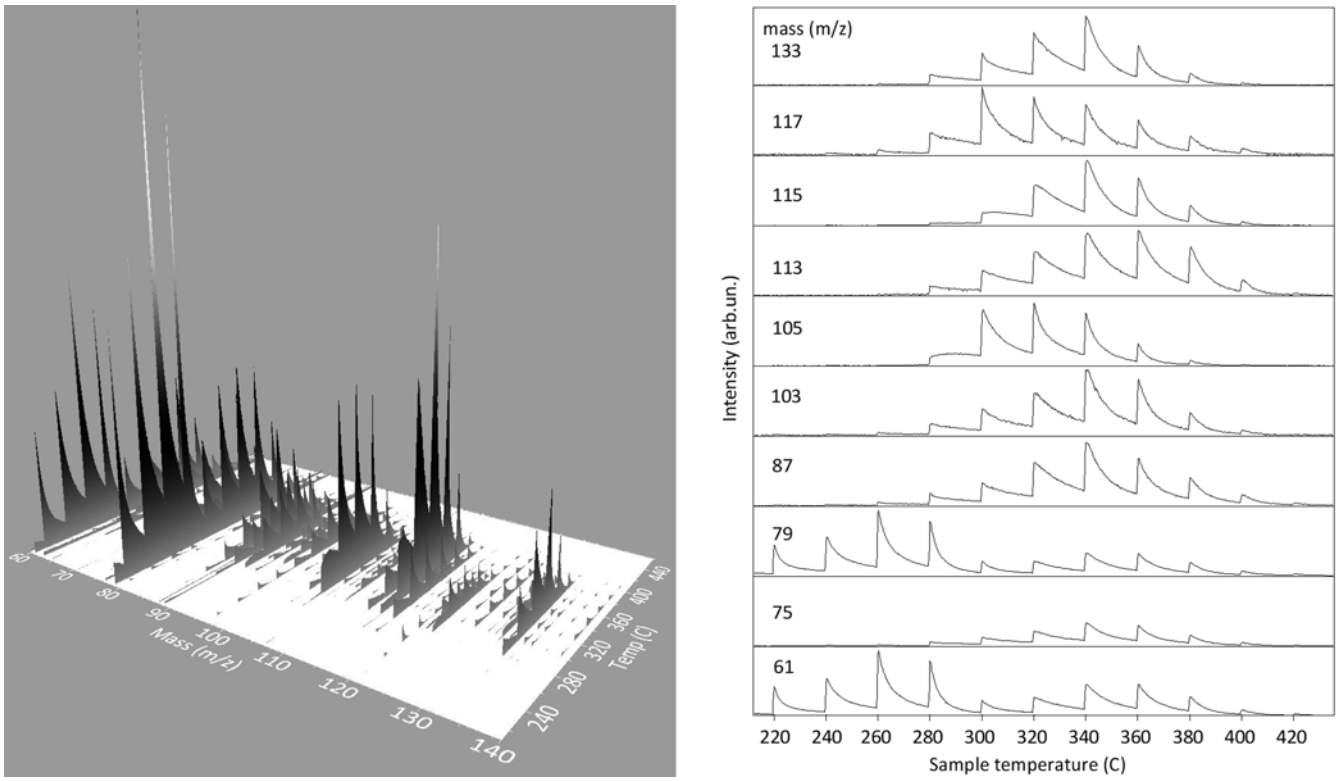

Figure 10. Left: Xylan multi-step pyrolysis from 220 to 460 °C, with steps of 20 °C lasting 40 s each. Right: Individual time profiles of the most abundant pyrolysis products. The integer *m*/*z* value is indicated for each profile.

1,4:3,6-dianhydro-α-D-glucopyranose. *m*/*z* 163 is levoglucosan. Unlike all of the others, which are protonated ions, *m*/*z* 180 is apparently merely ionized rather than protonated and is 4-(3-hydroxy-1-propenyl)-2-methoxyphenol, $C_{10}H_{12}O_3^+$

There is a pattern to this list of products. Cellulose is a linear polymer of hundreds or thousands of $C_6H_{10}O_5$ units. Each unit is a six-membered ring made up of one oxygen and five carbon atoms with a CH_3OH side chain, and each ring is attached to the next ring through an ether linkage. Many of the products consist of one of these rings, possibly after loss of one or more water molecules. Levoglucosan, for example, produces the *m*/*z* 163 ion when protonated and is made up of one $C_6H_{10}O_5$ unit, with the CH_3OH side chain having bonded across the O atom in the main ring to produce a second ring. Some of the products have reformed the ring, so that it has only four carbons and one oxygen (a tetrahydrofuran ring), with the extra carbon in a side chain. For example, 5-hydroxymethylfurfural, which produces the *m*/*z* 127 ion, is $C_6H_6O_3$; therefore, it has lost two water molecules and has a five-membered ring, with the extra carbon in a second side chain. Such dehydrated, possibly ring-reformed structures account for most of the major products. Only the smallest of the main products, *m*/*z* 61 and 79, are so small that they consist of only a fragment of a ring.

Xylan, a principal component of hemicellulose, was used for the hemicellulose tests because hemicellulose is not readily available commercially. The principal products observed from the multi-step pyrolysis of xylan are those shown in Figure 10. It shows that the pyrolysis proceeds in two waves, a low-temperature wave near 260 °C that produces the ions at *m*/*z* 61 and 79 and a higher temperature wave between 300 and 340 °C, in which most of the other ions in the figure are produced.

The pyrolysis of xylan has previously been studied;[17] therefore, many of the products have been identified. Half of the species plotted on the right in Figure 10 were included in the discussion of the 500 °C pyrolysis of poplar. The ions appearing in that previous discussion include the *m*/*z* 61 ion coming from acetic acid, *m*/*z* 79 produced by an ethanetriol or a dimethyl ether diol, *m*/*z* 103 from acetic anhydride or methyl pyruvate, *m*/*z* 113 coming from 2-furoic acid, and *m*/*z* 115 probably coming from either dihydro-2-(hydroxymethylene)-3(2*H*)-furanone or 4-hydroxy-5,6-dihydro-(2*H*)-pyran-2-

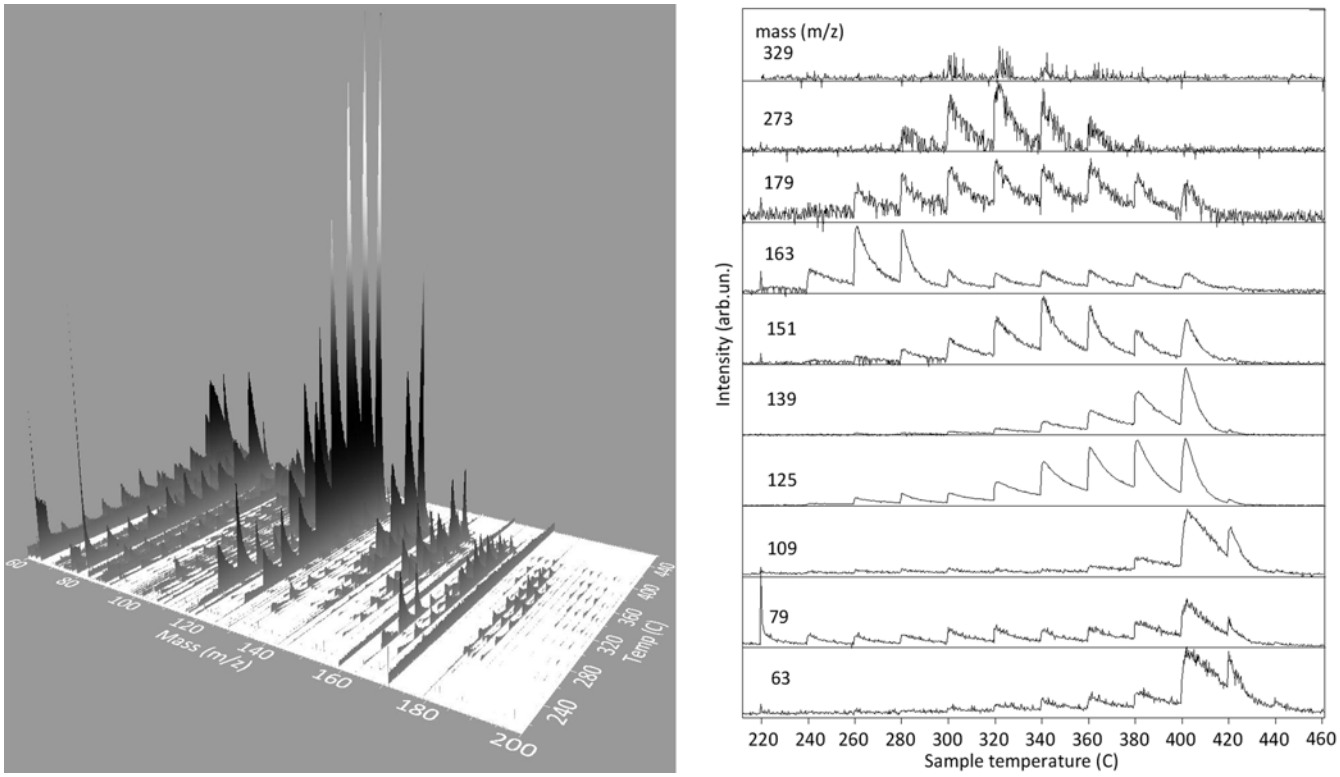

Figure 11. Left: Lignin multi-step pyrolysis from 220 to 460 °C, with steps of 20 °C lasting 40 s each. Right: Individual time profiles of the most abundant pyrolysis products. The integer *m*/*z* value is indicated for each profile.

one. The ions not previously discussed are *m*/*z* 75, 87, 105, 117, and 133. The *m*/*z* 75 ion is protonated $C_3H_6O_2$ and is probably propanoic acid, which has previously been identified as a pyrolysis product of xylan,[17] although acetol and 3-hydroxypropanal have the same formula and have also been observed in the pyrolysis of polysaccharides.[18,20,29] The *m*/*z* 87 ion probably comes from succindialdehyde or 2,3-dihydro-1,4-dioxin ($C_4H_6O_2$), both of which have been observed as products of xylan pyrolysis,[17] although butanedione[29] and dihydro-2(3*H*)-furanone[18] have also been observed in polysaccharide pyrolysis. The *m*/*z* 105 ion has an exact observed mass of 105.054 u, which corresponds to $[C_4H_8O_3 + H]^+$. This formula could be one of several different species, such as a methoxypropanoic acid or a hydroxybutanoic acid, which could be fragments of the xylose ring, but none of these have been observed as major products in xylan, hemicellulose, or wood pyrolysis. The *m*/*z* 117 ion is acetol acetate ($C_5H_8O_3$), which occurs in the pyrolysis of some hemicellulose components.[18,22,23,26] Lastly, the *m*/*z* 133 ion is 1-hydroxy-2-propanone acetate.[26]

The *m*/*z* 61 and 79 product ions occur in a low-temperature process, and their production peaks at approximately 260 °C. These are both small fragments of the xylose sugar ($C_5H_{10}O_5$) that makes up xylan. Their production at a temperature substantially below the temperatures at which they are produced from cellulose and at which other products come from xylan implies the presence of the open-chain form of the sugar, which is less stable than the usual closed ring. The other observed ions are produced at higher temperatures. Many of these are dehydration products either of the original xylose sugar and have formulas of the form $C_5H_{10-2x}O_{5-x}$ or of fragments of that sugar and have formulas of the form $C_{5-y}H_{10-2y-2x}O_{5-y-x}$. Some of the other products are deoxygenated derivatives of these dehydrated products with formulas of the form $C_{5-y}H_{10-2x-2y}O_{5-x-y-z}$. Dehydration and deoxygenation are typical steps in pyrolysis, and these results show that they are likely primary reactions and not secondary reactions of primary products.

Lignin is a much less uniform material than either cellulose or hemicellulose, and this is demonstrated by the plots in Figure 11 of the evolution of its pyrolysis products. Although lignin is generally considered to be the slowest wood component to pyrolyze, decomposing principally at higher

temperatures, the figure shows that products appear in substantial quantities from temperatures of 240 °C and up. The peak production of several ions in Figure 11 is at 400 °C, which is higher than the peak-production temperatures for any products from cellulose and hemicellulose, but the peak production of numerous other products are at lower temperatures.

Only a few of the ions in the right half of Figure 11 are major pyrolysis products from poplar. The *m*/*z* 79 ion, which is also observed in the pyrolysis of cellulose and hemicellulose, is likely an unstable species, probably an ethanetriol or dimethyl ether diol. The *m*/*z* 163 product, $(C_{10}H_{10}O_2 + H)^+$, is from lignin pyrolysis,[25,28] as previously noted.

Numerous products in Figure 11 are derivatives or variants of the guaiacol (2-methoxyphenol) structure that is the principal building block of softwood lignin. The *m*/*z* 125 ion is probably protonated guaiacol itself,[20,24,25,29] although the 3- and 4-methoxy isomers may also contribute.[19,21] The *m*/*z* 109 ion comes from methylphenol (C_7H_8O),[17,23,25] which is guaiacol after the loss of an oxygen. The *m*/*z* 139 ion is from either 3-methylguaiacol or 4-methylguaiacol ($C_8H_{10}O_2$).[17,24,25] The *m*/*z* 151 ion is 4-vinylguaiacol ($C_9H_{10}O_2$).[17,20,23-25,29] Coniferaldehyde ($C_{10}H_{10}O_3$), which could also be called 4-propenalguaiacol, is responsible for the *m*/*z* 179 product ion.[20,22,24,25,29]

The identities of the two largest ions plotted on the right in Figure 11 are not certain. The *m*/*z* 273 ion is protonated $C_{16}H_{16}O_4$, but the exact identity of this species has not been determined. Adams[22] identified it as 4,4'-dihydroxy-3,3'-dimethoxystilbene, while Evans et al.[33] have suggested that identity and two other structures as potential products, all of which involve two guaiacol units bound together by a two-carbon bridge. The exact observed mass of the *m*/*z* 329 ion is 329.140 u, which should correspond to $[C_{19}H_{20}O_5 + H]^+$. The identity of this species, however, has not been determined.

At the other end of the mass range is *m*/*z* 63, which probably comes from ethylene glycol ($HOCH_2CH_2OH$).

The correlation between the FTIR observations of the poplar char formation during stepwise pyrolysis with the MS observations of the components released by poplar during a similar stepwise pyrolysis provides useful information. Most of the species plotted on the right in Figure 8 reach their peak production level at the 350–370 °C steps, which is consistent with our observations that most of the infrared peaks of the wood are decreasing most rapidly in this same temperature range, as shown in Figure 4.

One exception to this pattern in Figure 8 is the *m*/*z* 193 species, whose production peaks at about 310 °C. The precise *m*/*z* for this ion is 193.087, which corresponds to protonated $C_{11}H_{12}O_3$ (see Table 2). Interestingly, a species with this formula has been associated with the pyrolysis of lignin,[24,28] but its peak production at relative low temperatures implies that its probable source is hemicellulose in our experiments. This is confirmed by our observation of the species among the major products of the pyrolysis of xylan, but not of the pyrolysis of lignin or cellulose. The identity of the *m*/*z* 193 cannot be pinned down precisely. There are many compounds having the formula $C_{11}H_{12}O_3$, but most involve a single benzene ring with one or two chains of atoms attached.

The parallel examination of the volatile products from poplar, cellulose, xylan, and lignin and of poplar char with multiple analytical techniques is a powerful approach to understand the processes underlying wood pyrolysis. Using DART-MS and FTIR-PAS has allowed us to identify the specific species produced during pyrolysis and their likely sources from among the components of wood.

Acknowledgment. This work was performed at Ames Laboratory, which is supported by the Office of Science, Office of Basic Energy Sciences, of the U.S. Department of Energy, under Contract DE-AC02-07CH11358 with the U.S. Department of Energy. This work was funded in part by the ConocoPhillips Company. We thank Dr. Monlin Kuo of Iowa State University for supplying the powdered and slab poplar used in this study.

Table 1: Sources of the Absorption Bands Whose Peak Heights Were Monitored as a Function of Pyrolysis Temperature[10]

wavenumber (cm^{-1})	source
3522	bond stretch of O–H hydrogen bonded to aromatic network[a]
3356	O–H bond stretch in cellulose, hemicellulose, and lignin
3055	C–H bond stretch in aromatic hydrocarbons
2932	C–H bond stretch in aliphatic hydrocarbons
1740	C=O bond stretch in xylan (part of hemicellulose)
1701	carbonyl band (tentative assignment)
1597	aromatic (benzene) ring stretch (only from lignin in fresh wood)
1504	aromatic (benzene) ring stretch in lignin
1373	CH_2 bending in both cellulose and hemicellulose
1327	CH_2 wagging vibration in cellulose
1238	mixed source; both syringyl nuclei in lignin and C=O in hemicellulose
1061	C=O bond stretch in both cellulose and hemicellulose

[a] From ref 14.

Table 2. Major Ions Observed in the 500 °C Pyrolysis of Poplar and Their Presence in the Pyrolysis of Individual Wood Components

poplar products		cellulose products		xylan products		lignin products		product identity		
observed mass (u)	relative size	observed mass (u)	relative size	observed mass (u)	relative size	observed mass (u)	relative size	Formula $[M + H]^+$	calculated mass (u)	most probable identity of M
61.030	32	61.027	21	61.028	62	61.027	23	$[C_2H_4O_2 + H]^+$	61.029	acetic acid
79.039	36	79.036	25	79.039	87	79.039	31	$[C_2H_6O_3 + H]^+$	79.040	ethane triol or dimethyl ether diol
85.027	33	85.026	36	85.027	8			$[C_4H_4O_2 + H]^+$	85.029	2(5*H*)-furanone
97.028	53	97.026	32	97.029	20			$[C_5H_4O_2 + H]^+$	97.029	2-furaldehyde
99.045	31	99.042	18	99.044	19			$[C_5H_6O_2 + H]^+$	99.045	furfuryl alcohol
103.041	30	103.038	24	103.039	22			$[C_4H_6O_3 + H]^+$	103.040	acetic anhydride and methyl pyruvate
111.044	35	111.042	12	111.044	6	111.044	23	$[C_6H_6O_2 + H]^+$	111.045	pyrocatechol and 2-acetyl furan
113.023	17	113.021	14	113.023	38			$[C_5H_4O_3 + H]^+$	113.024	2-furoic acid
115.039	62	115.036	20	115.039	100			$[C_5H_6O_3 + H]^+$	115.040	dihydro-2-(hydroxymethylene)-3(2*H*)-furanone or 4-hydroxy-5,6-dihydro-(2*H*)-pyran-2-one
127.038	71	127.036	62	127.038	9			$[C_6H_6O_3 + H]^+$	127.040	5-hydroxymethylfurfural
145.049	74	145.047	100					$[C_6H_8O_4 + H]^+$	145.050	1,4:3,6-dianhydro-α-D-glucopyranose
163.073	62	163.057	17	163.066	11	163.070	61	$[C_{10}H_{10}O_2 + H]^+$ or $[C_6H_{10}O_5 + H]^+$	163.076 or 163.061	4-propynylguaiacol or levoglucosan
179.071	16					179.070	22	$[C_{10}H_{10}O_3 + H]^+$	179.071	coniferaldehyde
180.087	15	180.084	12			180.086	14	$[C_{10}H_{12}O_3]^+$	180.079	coniferyl alcohol
193.087	100			193.080	8			$[C_{11}H_{12}O_3 + H]^+$	193.086	possibly 4-(4-hydroxy-3-

										methoxyphenyl)-3-butene-2-one
205.070	30	205.066	5					$[C_8H_{12}O_6 + H]^+$	205.071	not identified
209.080	28							$[C_{11}H_{12}O_4 + H]^+$	209.081	sinapaldehyde or 4-oxylallylsyringol
325.110	17	325.107	28					$[C_{12}H_{20}O_{10}+H]^+$	325.113	cellobiosan
342.138	15	342.133	19					$[C_{16}H_{22}O_8]^+$	342.131	possibly coniferin

REFERENCES

1. Mohan, D.; Pittman, C. U., Jr.; Steele, P. H. *Energy Fuels* **2006**, *20*, 848-889.

2. Babu, B. V. *Biofuels, Bioprod. Biorefin.* **2008**, *2*, 393-414.

3. Biagini, E.; Barontini, F.; Tognotti, L. *Ind. Eng. Chem. Res.* **2006**, *45*, 4486-4493.

4. Yang, H.; Yan, R.; Chen, H.; Lee, D. H.; Zheng, C. *Fuel* **2007**, *86*, 1781-1788.

5. Cody, R. B.; Laramée, J. A.; Durst, H. D. *Anal. Chem.* **2005**, *77*, 2297-2302.

6. Maleknia, S. D.; Bell, T. L.; Adams, M. A. *Int. J. Mass Spectrom.* **2009**, *279*, 126-133.

7. Michaelian, K. H. *Photoacoustic Infrared Spectroscopy*; Wiley-Interscience: Hoboken, NJ, 2003.

8. McClelland, J. F.; Jones, R. W.; Bajic, S. J. In *Handbook of Vibrational Spectroscopy*; Chalmers, J. M., Griffiths, P. R., Eds.; Wiley: Chichester, U.K., 2002; Vol. 2, pp 1231-1251.

9. Bajic, S. J.; Jones, R. W.; McClelland, J. F.; Hames, B. R.; Meglen, R. R. In *Fourier Transform Spectroscopy: Eleventh International Conference*; de Haseth, J. A., Ed.; American Institute of Physics (AIP): Woodbury, NY, 1998; AIP Conference Proceeding 430, pp 466-469.

10. Kuo, M.-L.; McClelland, J. F.; Luo, S.; Chien, P.-L.; Walker, R. D.; Hse, C.-Y. *Wood Fiber Sci.* **1988**, *20*, 132-145.

11. Pandey, K. K.; Theagarajan, K. S. *Holz Roh- Werkst.* **1997**, *55*, 383-390.

12. Brewer, C. E.; Schmidt-Rohr, K.; Satrio, J. A.; Brown, R. C. *Environ. Prog. Sustainable Energy* **2009**, *28*, 386-396.

13. On the basis of data from http://www.matbase.com/material/wood/class5-5-years/poplar/properties.

14. Herring, A. M.; McKinnon, J. T.; Gneshin, K. W.; Pavelka, R.; Petrick, D. E.; McCloskey, B. D.; Filley, J. *Fuel* **2004**, *83*, 1483-1494.

15. Bilba, K.; Ouensanga, A. *J. Anal. Appl. Pyrolysis* **1996**, *38*, 61-73.

16. Boon, J. J.; Pastorova, I.; Botto, R. E.; Arisz, P. W. *Biomass Bioenergy* **1994**, *7*, 25-32.

17. Nowakowski, D. J.; Woodbridge, C. R.; Jones, J. M. *J. Anal. Appl. Pyrolysis* **2008**, *83*, 197-204.

18. Aho, A.; Kumar, N.; Eränen, K.; Holmbom, B.; Hupa, M.; Salmi, T.; Murzin, D. Y. *Int. J. Mol. Sci.* **2008**, *9*, 1665-1675.

19. Marsman, J. H.; Wildschut, J.; Mahfud, F.; Heeres, H. J. *J. Chromatogr. A* **2007**, *1150*, 21-27.

20. Hosoya, T.; Kawamoto, H.; Saka, S. *J. Wood Sci.* **2007**, *53*, 351-357.

21. Marsman, J. H.; Wildschut, J.; Evers, P.; de Koning, S.; Heeres, H. J. *J. Chromatog. A* **2008**, *1188*, 17-25.

22. Adams, J. *Int. J. Mass Spectrom.* **2010**. DOI: 10.1016/j.ijms.2010.07.025.

23. Wang, X.; Chen, H.; Luo, K.; Shao, J.; Yang, H. *Energy Fuels* **2008**, *22*, 67-74.

24. Butt, D. *Thermochemical Processing of Agroforestry Biomass for Furans, Phenols, Cellulose and Essential Oils*; Rural Industries Research and Development Corporation (RIRDC): Kingston, Australian Capital Territory, Australia, 2006; Publication 06/121.

25. Ralph, J.; Hatfield, R. D. *J. Agric. Food Chem.* **1991**, *39*, 1426-1437.

26. Evans, R. J.; Milne, T. A. *Energy Fuels* **1987**, *1*, 123-137.

27. Šimkovic, I.; Alföldi, J.; Schulten, H.-R. *Biomass Bioenergy* **1993**, *4*, 373-378.

28. Oudia, A,; Mészáros, E.; Jakab, E.; Simões, R.; Queiroz, J.; Ragauskas, A.; Novák, L. *J. Anal. Appl. Pyrolysis* **2009**, *85*, 19-29.

29. Popescu, C.-M.; Dobele, G.; Rossinskaja, G.; Dizhbite, T.; Vasile, C. *J. Anal. Appl. Pyrolysis* **2007**, *79*, 71-77.

30. Gutiérrez, A.; Rodríguez, I. M.; del Río, J. C. *J. Agric. Food Chem.* **2004**, *52*, 4764-4773.

31. Sharma, R. K.; Wooten, J. B.; Baliga, V. L.; Lin, X.; Chan, W. G.; Hajaligol, M. R. *Fuel* **2004**, *83*, 1469-1482.

32. Chaiwat, W.; Hasegawa, I.; Tani, T.; Sunagawa, K.; Mae, K. *Energy Fuels* **2009**, *23*, 5765-5772.

33. Evans, R. J.; Milne, T. A.; Soltys, M. N. *J. Anal. Appl. Pyrolysis* **1986**, *9*, 207-236.